

Universal bound to the amplitude of the vortex Nernst signal in superconductors

Carl Willem Rischau^{1,*}, Yuke Li^{1,†}, Benoît Fauqué^{2,‡}, Hisashi Inoue^{3,‡}, Minu Kim^{3,§},
Christopher Bell^{3,¶}, Harold Y. Hwang³, Aharon Kapitulnik³, and Kamran Behnia^{1,**}

(1) *Laboratoire de Physique et d'étude des Matériaux
(ESPCI Paris - CNRS - Sorbonne Université),
PSL Research University, 75005 Paris, France*
(2) *JEIP, USR 3573 CNRS, Collège de France,
PSL Research University, 75005, Paris France*
(3) *Geballe Laboratory for Advanced Materials,
Stanford University, Stanford, CA 94305, USA*

(Dated: December 22, 2024)

A liquid of superconducting vortices generates a transverse thermoelectric response. This Nernst signal has a tail deep in the normal state due to superconducting fluctuations. Here, we present a study of the Nernst effect in two-dimensional hetero-structures of Nb-doped strontium titanate and in amorphous MoGe. The Nernst signal generated by ephemeral Cooper pairs above the critical temperature has the magnitude expected by theory. On the other hand, the peak amplitude of the vortex Nernst signal below T_c is unexpectedly comparable ($\approx 0.1 k_B/e$) in both. We show that this is also the case of all superconductors hitherto explored, in spite of the variety of their critical temperatures (distributed over three orders of magnitude). This upper boundary to the Nernst response implies a lower boundary to the ratio of viscosity to entropy density of vortex liquids.

Superconducting vortices are quanta of magnetic flux with a normal core surrounded by a whirling flow of Cooper pairs [1]. In a ‘vortex liquid’ a charge current and an electric field can be simultaneously present and produce dissipation. This state of matter is prominent in high- T_c cuprates [2]. One property of the vortex liquid is a finite Nernst effect (the generation of a transverse electric field by a longitudinal thermal gradient) [3]. Together with its Etingshausen counterpart (a transverse thermal gradient produced by a longitudinal charge current), it has been widely documented in both conventional [4] and high- T_c superconductors [5–7]. In the latter case, the debate has been mostly focused on interpreting the persistence of a Nernst signal above the critical temperature [7–9]. The vortex origin of the peak signal below T_c remains undisputed and its quantitative amplitude unexplained. Theoretical tradition has linked the magnitude of the finite Nernst signal to the motion of vortices under the influence of a thermal gradient due to the excess entropy of the normal core [4, 10–12]. As a consequence, the magnitude of the Nernst response is

expected to strongly vary among different superconductors [10–12].

Here we present a study of the Nernst effect in two superconductors, namely two-dimensional Nb-doped SrTiO₃ and α -MoGe. We will show that the magnitude of the fluctuating Nernst response above T_c is in agreement with theoretical expectations. On the other hand, the amplitude of the vortex Nernst signal in the flux flow regime below the critical temperature cannot be explained by the traditional approach. Then, putting under scrutiny the data for other superconductors studied until present (with a range of critical temperatures extending over three orders of magnitude), we find that the observed peak is always a few $\mu\text{V}/\text{K}$. We will argue that this implies a lower bound to the ratio of the viscous friction coefficient to the entropy density in vortex liquids. We note that a bound to the viscosity-entropy ratio was proposed in the context of strongly interacting quantum field theories [13] and exists in common liquids [14].

Fig. 1 presents our data on two-dimensional Nb-doped strontium titanate (STO). The heterostructure consisted of 1% at. Nb:SrTiO₃ ($n_{2D} = 8.6 \times 10^{13} \text{cm}^{-2}$) with thickness of 4.5 nm sandwiched by cap and buffer undoped STO layers (see Fig. 1a). Previous studies documented the normal-state [15, 16] and the superconducting properties [17] of such δ -doped samples in detail. Using a standard two-thermometers-one-heater set-up (see Fig. 1b), we measured diagonal (resistivity and thermopower) as well as off-diagonal (Nernst and Hall effects) transport coefficients of the sample with the same electrodes (see the supplement [18] for more details). As seen in panels d-j of the same figure, a Nernst signal emerges in the vortex state and its peak shifts with magnetic field and remains close to the midpoint of the resistive transition.

*Present address: Department of Quantum Matter Physics, University of Geneva, 1205 Geneva, Switzerland

†Present address: Department of Physics & Hangzhou Key Laboratory of Quantum Matter, Hangzhou Normal University, Hangzhou, 311121, China

‡Present address: Frontier Research Institute for Interdisciplinary Sciences and Institute for Materials Research, Tohoku University, Sendai 980-8577, Japan

§Present address: Max Planck Institute for Solid State Research, Heisenbergstrasse 1, 70569 Stuttgart, Germany

¶Present address: H. H. Wills Physics Laboratory, University of Bristol, Tyndall Avenue, Bristol, BS8 1TL, UK

**Electronic address: kamran.behnia@espci.fr

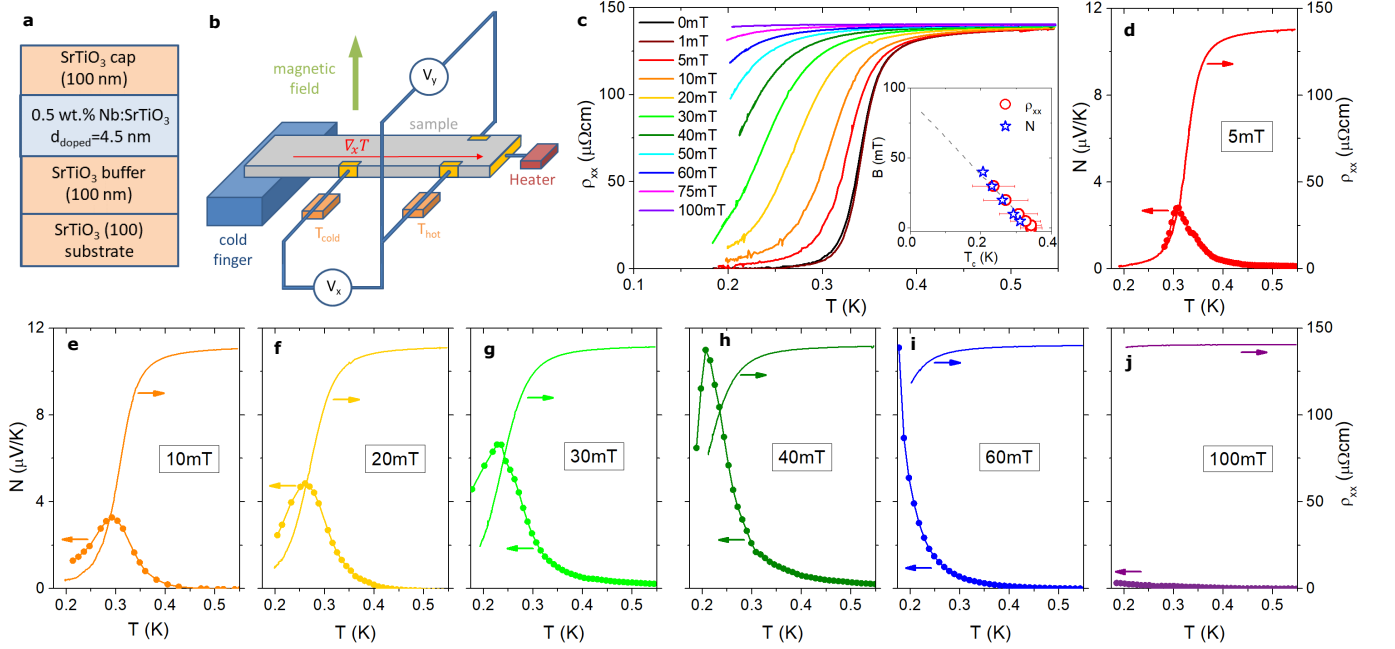


FIG. 1: **Nernst effect in two-dimensional Nb-doped strontium titanate:** a) Schematic view of the heterostructure. b) Sketch of the two-thermometers-one-heater set-up used in these measurements. c) Resistivity ρ_{xx} as a function of temperature. The midpoint resistive transition at $T_c = 0.341$ K shifts to lower temperatures with increasing magnetic field. The inset shows the correlated evolution of this midpoint and the Nernst peak with temperature and magnetic field. d-j) The Nernst signal N and ρ_{xx} vs. temperature at different magnetic fields, both the Nernst peak and the resistive transition vanish at $B = 0.1$ T.

Fig. 2a shows the evolution of the low-field Nernst coefficient ($\nu = N/B$) across T_c . Its magnitude is extremely sensitive to magnetic field. The Nernst coefficient of the normal quasi-particles detected in bulk crystals of doped STO [22] is much smaller and has an opposite sign ($\nu = -0.04 \mu\text{V}/\text{KT}$ at $B = 1$ T and $T = 0.5$ K) [3, 22]. It is negligible at $B = 0.005$ T. As indicated by a recent study on NbSe₂ [23], confinement to two dimensions facilitates the observation of the superconducting contribution to the Nernst response.

Theoretically, the Nernst signal due to the Gaussian fluctuations of the superconducting order parameter [24–26] leads to a simple expression for the off-diagonal component of the thermoelectric tensor, α_{xy} :

$$\frac{\alpha_{xy}^{Fl}}{B}(T) = \frac{k_B e^2}{6\pi\hbar^2} \xi^2(T). \quad (1)$$

Here, $\xi(T) = \xi_0/\sqrt{\epsilon}$ is the superconducting coherence length and $\epsilon = (T - T_c)/T_c$ is the reduced temperature. Combining our Nernst and resistivity data, we can plot α_{xy} in Fig. 2b. Its magnitude at twice T_c is compatible with what is expected by Eq. 1 and the zero-temperature coherence length extracted from the upper critical field ($\xi_0 = 60$ nm) [15]. Similar observations were previously reported for amorphous superconductors [19, 27, 28] and in cuprates [20, 21]. Because of the long ξ , α_{xy} found here is larger than those studied previously (See the inset in Fig. 2b and the supplement [18]).

We now turn our attention to the vortex Nernst signal

below the critical temperature. The maximum Nernst signal in Nb:STO is $N = 11 \mu\text{V}/\text{K}$ at $B = 0.04$ T and $T = 0.2$ K. At this temperature and magnetic field, the measured resistivity is $75 \mu\Omega\text{cm}$. Thus, the peak transverse thermoelectric response is $\alpha_{xy} = N/\rho = 14.6$ A/Km. In the traditional approach [3, 4, 6], this is set by a balance between the thermal force (set by the entropy of each vortex, S_d) and the Lorentz force (set on its magnetic flux, ϕ_0). With $\phi_0 = h/2e = 2.07 \times 10^{-15}$ Tm² [1], one finds $S_d = 3 \times 10^{-14}$ J/K. m. As discussed in the supplement [18], this falls well below the theoretically expected S_d [12].

Fig. 3 presents a study of the Nernst effect in another two-dimensional superconductor, namely amorphous MoGe, a platform for studying superconductor-insulator transitions [32]. The Nernst peak evolves concomitantly with the resistive transition with increasing magnetic field. The magnitude of the vortex Nernst signal observed here is comparable to other two-dimensional amorphous films studied before, such as NbSi [27] or InO_x [28, 33]. Note also that the Nernst signal in MoGe is only slightly lower than in Nb: STO. Since resistivity is also a bit smaller at this Nernst peak, the extracted α_{xy} (≈ 14 A/Km) and S_d ($\approx 2.8 \times 10^{-14}$ J/K.m) are virtually identical in the two systems, in spite of an almost 20-fold difference in T_c (6.2 K vs. 0.34 K).

This brings us to a hitherto unnoticed experimental fact. The Nernst signal ($N = S_{xy} = \frac{E_y}{\nabla_x T}$) peaks to comparable magnitude in all known superconductors. This

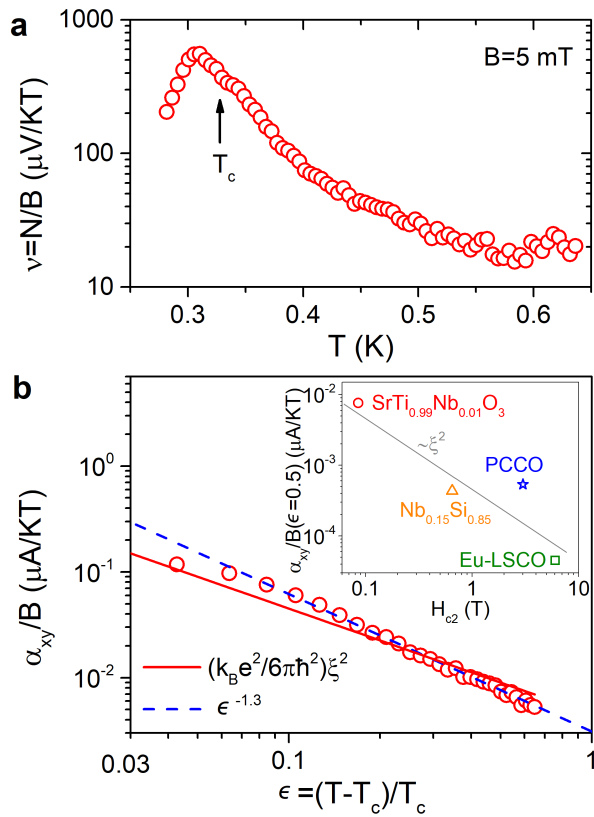


FIG. 2: **Nernst response in the normal state due to superconducting fluctuations:** a) The Nernst coefficient as a function of temperature in two-dimensional Nb:STO across the critical temperature at $B = 5$ mT. b) The off-diagonal component of the thermoelectric tensor, $\alpha_{xy} = \frac{N}{\rho} a_0$ as a function of reduced temperature, $\epsilon = (T - T_c)/T_c$. The dashed line represents $\epsilon^{-1.3}$, the solid line what is expected by Eq. 1. The inset compares the magnitude of normal-state α_{xy} (at $T = 1.5T_c$) in different superconductors [19–21] as a function of their upper critical field, H_{c2} . The dashed line represents the magnitude expected by Eq. 1 and a coherence length given by $H_{c2}(0)$.

is illustrated in Fig.4. Available data on cuprate, iron-based, organic and amorphous superconductors indicate that the peak Nernst signal is also of the order of a few $\mu\text{V}/\text{K}$ (Fig. 4a). In bulk conventional superconductors, the vortex liquid is restricted to a narrow field window and we could not find any published report of $N(T)$ data at fixed magnetic field. Nevertheless, the order of magnitude of the signals is similar [4]. A very recent study [23] quantified the Nernst peak of two-dimensional crystalline NbSe to be $\sim 5 \mu\text{V}/\text{K}$. Figs. 4b-d compares the contours of $N(T, B)$ in three different superconductors. The field and temperature scales differ by two orders of magnitude, but the summit is always a few $\mu\text{V}/\text{K}$.

Note that this universality is specific to the vortex Nernst response. The magnitude of the Ettingshausen coefficient, which arises when vortices move by a Lorentz force is *not* universal (see the supplement [18]). It is

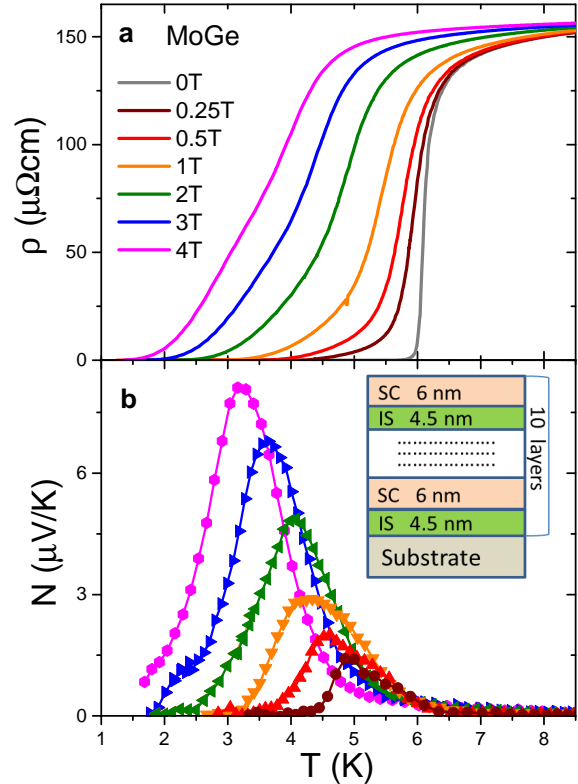


FIG. 3: **Nernst effect in amorphous MoGe:** a) Evolution of the resistive superconducting transition in amorphous films of MoGe with magnetic field. b) Nernst effect N in the same sample. The color code for magnetic fields is identical to the one used in the upper panel. The inset schematically depicts the structure of the sample consisting of alternating superconducting and insulating layers.

also worth to highlight the contrast with the Nernst signal generated by quasi-particles of a Fermi liquid set by the ratio of mobility and the Fermi energy. The available data spreads over more than six orders of magnitude [3, 8]. In this context, the quasi-identical magnitude of the peak vortex Nernst signal is puzzling and, given the large variety of material-dependent parameters, is unexpected in the traditional approach.

Let us briefly sketch the widely used picture of the vortex Nernst response. A thermal gradient generates a thermal force on each vortex. This force is balanced by a damping force leading to a steady displacement of vortices. The finite vortex velocity will generate a phase slip along the perpendicular orientation and, thanks to the Josephson equation, a finite electric field. Now, the thermal force on a vortex with an entropy of S_d is countered by a damping force proportional to the velocity of the vortex line v_L and a viscous parameter η' [4]:

$$S_d \vec{\nabla}_x T = \eta' \vec{v}_L \quad (2)$$

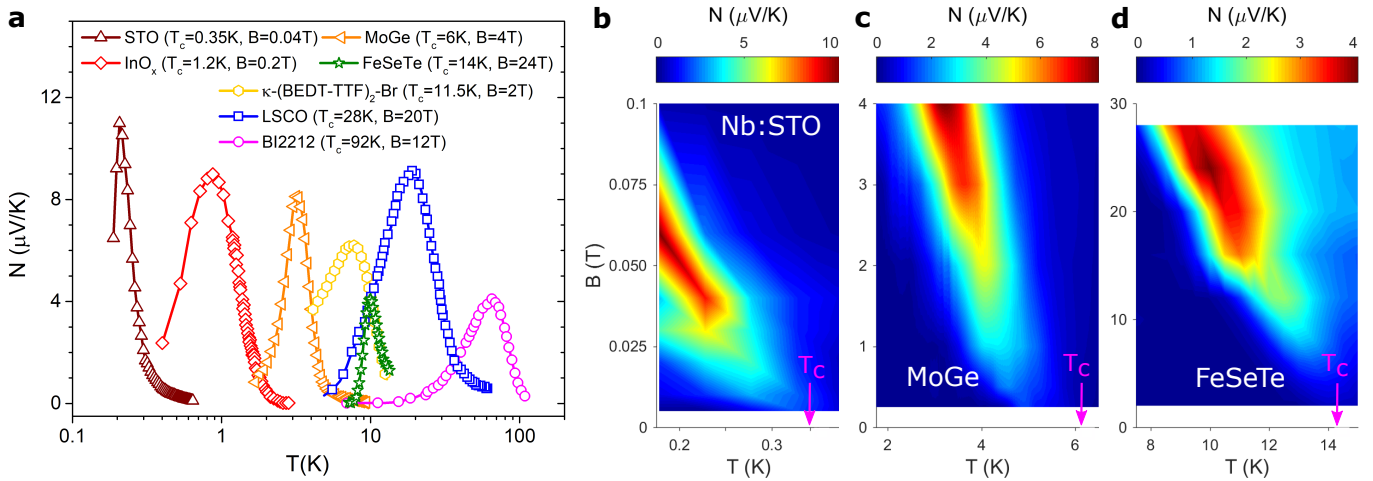


FIG. 4: **Peak Nernst signal in different superconductors:** a) The Nernst signal as a function of temperature in STO and MoGe (present work) compared with data on an amorphous film of InO_x [28], on $\text{FeSe}_{0.6}\text{Te}_{0.4}$ [29], on $\kappa\text{-(BEDT-TTF)}_2\text{Cu}[\text{N}(\text{CN})_2\text{Br}$ [30], on $\text{La}_{1.92}\text{Sr}_{0.08}\text{CuO}_4$ [31] and on $\text{Bi}_2\text{Sr}_2\text{CaCu}_2\text{O}_{8+\delta}$ [6]. For each system, the critical temperature is indicated together with the magnetic field at which the observed peak was the largest. In all systems, this magnetic field is the one at which the peak is largest, except in Bi2212 [6], for which the data was restricted to 12 T. The field and temperature dependence of the Nernst signal are shown as color plots for b) Nb:STO, c) MoGe and d) $\text{FeSe}_{0.6}\text{Te}_{0.4}$ [29]. Note the similarity in the peak amplitude in contrast to the large difference in the field and temperature scales.

A steady motion of vortices would generate a temporal variation of the superconducting phase along the orientation perpendicular to the vortex movement. With each vortex carrying a magnetic flux of $\phi_0 = \frac{h}{2e}$ and their density equal to n_V , the Josephson equation leads to :

$$\vec{E} = \vec{v}_L \times n_V \frac{h}{2e} \hat{z} \quad (3)$$

By combining the two equations and introducing the entropy density $s = \frac{S_d}{n_V}$, one finds:

$$N \equiv \frac{E_y}{\nabla_x T} = \frac{h}{2e} \frac{s}{\eta'} \quad (4)$$

Thus, the Nernst signal is set by the ratio of entropy density to the viscous parameter η' . The traditional approach [3, 4, 6] assumes that this η' is identical to the damping parameter opposing the Lorentz force in the flux flow resistivity and therefore $S_d = \phi_0 N / \rho$. Our finding, however, invites a serious re-examination of this picture.

A more sophisticated approach would consider momentum exchange between three subsystems: the superfluid ‘vacuum’ [34], the normal quasi-particles and the topological texture introduced by the presence of vortices. The balance of all dissipative and reactive forces on a vortex [34–36] would lead to :

$$\hat{z} \times (\vec{v}_L - \vec{v}_s) + d_\perp \hat{z} \times (\vec{v}_n - \vec{v}_L) + d_\parallel (\vec{v}_n - \vec{v}_L) = 0 \quad (5)$$

This expression includes the Magnus force between the vortex and the superfluid (which has a velocity of v_s), the Iordanskii force (proportional to the differential velocity of the normal fluid v_n and the superfluid) and the

Kopnin force (proportional to the differential velocity of the normal fluid and the vortex), which is a consequence of spectral flow [35, 37] in fermionic superfluids. The two dimensionless parameters d_\perp and d_\parallel represent dissipation and quantify the viscous response. Now, the Lorentz force generated by a charge current and a thermal force generated by a thermal gradient do not affect the three velocities in the same way. Therefore, the dissipation they cause and the associated η' are not necessarily identical. The viscous parameter, η' , first introduced by Bardeen and Stephen to quantify flux flow resistivity [38] is to be distinguished from the dynamic viscosity, η of a compressible fluid. While η' is the ratio of the force to velocity, η is ratio of the force to the gradient of velocity. In the vortex liquid, the spatial modulation of v_n and v_s near the cores [1, 37, 38] opens room for genuine viscosity of compressible liquids.

According to available experimental data, the vortex Nernst peak remains below $11 \mu\text{V}/\text{K} \approx k_B/8e$. Combining this with Eq. 4, leads us to:

$$\frac{\eta'}{s} > c_{vo} \frac{\hbar}{k_B} \quad (6)$$

Empirically, $c_{vo} \approx 8\pi$. A boundary to η/s was put forward in quantum field theory [13] and is detectable in common liquids [14] (see the supplement [18] for the data on H_2O and helium). This provides another motivation to quantify η and clarify its link to η' .

We thank H. Aubin, M. V. Feigel'man, S. A. Hartnoll, S. A. Kivelson K. Trachenko A. A. Varlamov and G. E. Volovik for discussions. CWR acknowledges the support of Fonds-ESPCI, Paris. This work was supported by a QuantEmX Exchange Awards at Stanford University

(KB) and at ESPCI (AK). In France, it was supported by the Agence Nationale de la Recherche (ANR-18-CE92-0020-01; ANR-19-CE30-0014-04) and by Jeunes Equipes de l'Institut de Physique du Collège de France. HI, MK, CB, and HYH were supported by the U.S. Department of

Energy, Office of Basic Energy Sciences, Division of Materials Sciences and Engineering, under contract no. DE-AC02-76SF00515. AK was supported by the National Science Foundation Grant NSF-DMR-1808385.

-
- [1] M. Tinkham, *Introduction to superconductivity* (Courier Corporation, 1996).
- [2] G. Blatter, M. V. Feigel'man, V. B. Geshkenbein, A. I. Larkin, and V. M. Vinokur, *Rev. Mod. Phys.* **66**, 1125 (1994), URL <https://link.aps.org/doi/10.1103/RevModPhys.66.1125>.
- [3] K. Behnia and H. Aubin, *Rep. Prog. Phys.* **79**, 046502 (2016), URL <http://stacks.iop.org/0034-4885/79/i=4/a=046502>.
- [4] R. P. Huebener, *Magnetic Flux Structures in Superconductors* (Springer-Verlag, Berlin, 1979).
- [5] T. T. M. Palstra, B. Batlogg, L. F. Schneemeyer, and J. V. Waszczak, *Phys. Rev. Lett.* **64**, 3090 (1990), URL <https://link.aps.org/doi/10.1103/PhysRevLett.64.3090>.
- [6] H.-C. Ri, R. Gross, F. Gollnik, A. Beck, R. P. Huebener, P. Wagner, and H. Adrian, *Phys. Rev. B* **50**, 3312 (1994), URL <https://link.aps.org/doi/10.1103/PhysRevB.50.3312>.
- [7] Y. Wang, L. Li, and N. P. Ong, *Phys. Rev. B* **73**, 024510 (2006), URL <https://link.aps.org/doi/10.1103/PhysRevB.73.024510>.
- [8] K. Behnia, *Journal of Physics: Condensed Matter* **21**, 113101 (2009), URL <http://stacks.iop.org/0953-8984/21/i=11/a=113101>.
- [9] O. Cyr-Choinière, R. Daou, F. Laliberté, C. Collignon, S. Badoux, D. LeBoeuf, J. Chang, B. J. Ramshaw, D. A. Bonn, W. N. Hardy, et al., *Phys. Rev. B* **97**, 064502 (2018), URL <https://link.aps.org/doi/10.1103/PhysRevB.97.064502>.
- [10] M. J. Stephen, *Phys. Rev. Lett.* **16**, 801 (1966), URL <https://link.aps.org/doi/10.1103/PhysRevLett.16.801>.
- [11] K. Maki, *Physica* **55**, 124 (1971), ISSN 0031-8914, URL <http://www.sciencedirect.com/science/article/pii/0031891471902473>.
- [12] A. Sergeev, M. Reizer, and V. Mitin, *EPL (Europhysics Letters)* **92**, 27003 (2010), URL <https://doi.org/10.1209/2F0295-5075/2F92/2F27003>.
- [13] P. K. Kovtun, D. T. Son, and A. O. Starinets, *Phys. Rev. Lett.* **94**, 111601 (2005), URL <https://link.aps.org/doi/10.1103/PhysRevLett.94.111601>.
- [14] K. Trachenko and V. V. Brazhkin, *Science Advances* **6** (2020).
- [15] Y. Kozuka, M. Kim, C. Bell, B. G. Kim, Y. Hikita, and H. Y. Hwang, *Nature* **462**, 487 (2009), ISSN 1476-4687, URL <https://doi.org/10.1038/nature08566>.
- [16] M. Kim, C. Bell, Y. Kozuka, M. Kurita, Y. Hikita, and H. Y. Hwang, *Phys. Rev. Lett.* **107**, 106801 (2011), URL <https://link.aps.org/doi/10.1103/PhysRevLett.107.106801>.
- [17] M. Kim, Y. Kozuka, C. Bell, Y. Hikita, and H. Y. Hwang, *Phys. Rev. B* **86**, 085121 (2012), URL <https://link.aps.org/doi/10.1103/PhysRevB.86.085121>.
- [18] See Supplemental Material for more details.
- [19] A. Pourret, H. Aubin, J. Lesueur, C. A. Marrache-Kikuchi, L. Bergé, L. Dumoulin, and K. Behnia, *Nature Physics* **2**, 683 (2006), ISSN 1745-2481, URL <https://doi.org/10.1038/nphys413>.
- [20] J. Chang, N. Doiron-Leyraud, O. Cyr-Choinière, G. Grissonnanche, F. Laliberté, E. Hassinger, J.-P. Reid, R. Daou, S. Pyon, T. Takayama, et al., *Nature Phys* **8**, 751 (2012).
- [21] F. F. Tafti, F. Laliberté, M. Dion, J. Gaudet, P. Fournier, and L. Taillefer, *Phys. Rev. B* **90**, 024519 (2014), URL <https://link.aps.org/doi/10.1103/PhysRevB.90.024519>.
- [22] X. Lin, Z. Zhu, B. Fauqué, and K. Behnia, *Phys. Rev. X* **3**, 021002 (2013), URL <https://link.aps.org/doi/10.1103/PhysRevX.3.021002>.
- [23] X.-Q. Li, Z.-L. Li, J.-J. Zhao, and X.-S. Wu, *Chinese Physics B* (2020), URL <http://iopscience.iop.org/10.1088/1674-1056/ab9614>.
- [24] I. Ussishkin, S. L. Sondhi, and D. A. Huse, *Phys. Rev. Lett.* **89**, 287001 (2002), URL <https://link.aps.org/doi/10.1103/PhysRevLett.89.287001>.
- [25] M. N. Serbyn, M. A. Skvortsov, A. A. Varlamov, and V. Galitski, *Phys. Rev. Lett.* **102**, 067001 (2009), URL <https://link.aps.org/doi/10.1103/PhysRevLett.102.067001>.
- [26] K. Michaeli and A. M. Finkel'stein, *EPL (Europhysics Letters)* **86**, 27007 (2009), URL <https://doi.org/10.1209/2F0295-5075/2F86/2F27007>.
- [27] A. Pourret, H. Aubin, J. Lesueur, C. A. Marrache-Kikuchi, L. Bergé, L. Dumoulin, and K. Behnia, *Phys. Rev. B* **76**, 214504 (2007), URL <https://link.aps.org/doi/10.1103/PhysRevB.76.214504>.
- [28] P. Spathis, H. Aubin, A. Pourret, and K. Behnia, *EPL (Europhysics Letters)* **83**, 57005 (2008), URL <https://doi.org/10.1209/2F0295-5075/2F83/2F57005>.
- [29] A. Pourret, L. Malone, A. B. Antunes, C. S. Yadav, P. L. Paulose, B. Fauqué, and K. Behnia, *Phys. Rev. B* **83**, 020504 (2011), URL <https://link.aps.org/doi/10.1103/PhysRevB.83.020504>.
- [30] G. Y. Logvenov, M. V. Kartsovnik, H. Ito, and T. Ishiguro, *Synthetic Metals* **86**, 2023 (1997).
- [31] C. Capan, K. Behnia, J. Hinderer, A. G. M. Jansen, W. Lang, C. Marcenat, C. Marin, and J. Flouquet, *Phys. Rev. Lett.* **88**, 056601 (2002), URL <https://link.aps.org/doi/10.1103/PhysRevLett.88.056601>.
- [32] A. Yazdani and A. Kapitulnik, *Phys. Rev. Lett.* **74**, 3037 (1995), URL <https://link.aps.org/doi/10.1103/PhysRevLett.74.3037>.
- [33] A. Roy, E. Shimshoni, and A. Frydman, *Phys. Rev. Lett.* **121**, 047003 (2018), URL <https://link.aps.org/doi/10.1103/PhysRevLett.121.047003>.
- [34] G. E. Volovik, *The Universe in a Helium Droplet* (Oxford University Press, 2003), ISBN 0198507828, URL <https://doi.org/10.1093/0198507828>.

- //www.oxfordscholarship.com/10.1093/acprof:oso/9780199564842.001.0001/acprof-9780199564842.
- [35] N. B. Kopnin, G. E. Volovik, and Ü. Parts, *Europhysics Letters (EPL)* **32**, 651 (1995), URL <https://doi.org/10.1209/2F0295-5075%2F32%2F8%2F006>.
- [36] E. B. Sonin, *Phys. Rev. B* **55**, 485 (1997), URL <https://link.aps.org/doi/10.1103/PhysRevB.55.485>.
- [37] C. Caroli, P. D. Gennes, and J. Matricon, *Physics Letters* **9**, 307 (1964), ISSN 0031-9163, URL <http://www.sciencedirect.com/science/article/pii/0031916364903750>.
- [38] J. Bardeen and M. J. Stephen, *Phys. Rev.* **140**, A1197 (1965), URL <https://link.aps.org/doi/10.1103/PhysRev.140.A1197>.
- [39] V. Martelli, J. L. Jiménez, M. Continentino, E. Baggio-Saitovitch, and K. Behnia, *Phys. Rev. Lett.* **120**, 125901 (2018), URL <https://link.aps.org/doi/10.1103/PhysRevLett.120.125901>.
- [40] A. Pourret, P. Spathis, H. Aubin, and K. Behnia, *New Journal of Physics* **11**, 055071 (2009), URL <https://doi.org/10.1088%2F1367-2630%2F11%2F5%2F055071>.
- [41] A. Larkin and A. Varlamov, *Theory of Fluctuations in Superconductors* (Clarendon, Clarendon, 2005).
- [42] M. R. Cimberle, C. Ferdeghini, E. Giannini, D. Marré, M. Putti, A. Siri, F. Federici, and A. Varlamov, *Phys. Rev. B* **55**, R14745 (1997), URL <https://link.aps.org/doi/10.1103/PhysRevB.55.R14745>.
- [43] X. Lin, G. Bridoux, A. Gourgout, G. Seyfarth, S. Krämer, M. Nardone, B. Fauqué, and K. Behnia, *Phys. Rev. Lett.* **112**, 207002 (2014), URL <https://link.aps.org/doi/10.1103/PhysRevLett.112.207002>.
- [44] C. Collignon, B. Fauqué, A. Cavanna, U. Gennser, D. Mailly, and K. Behnia, *Phys. Rev. B* **96**, 224506 (2017), URL <https://link.aps.org/doi/10.1103/PhysRevB.96.224506>.
- [45] X. F. Sun, J. Takeya, S. Komiya, and Y. Ando, *Phys. Rev. B* **67**, 104503 (2003), URL <https://link.aps.org/doi/10.1103/PhysRevB.67.104503>.
- [46] X. Lin, A. Gourgout, G. Bridoux, F. Jomard, A. Pourret, B. Fauqué, D. Aoki, and K. Behnia, *Phys. Rev. B* **90**, 140508 (2014), URL <https://link.aps.org/doi/10.1103/PhysRevB.90.140508>.
- [47] P. W. Bridgman, *Phys. Rev.* **24**, 644 (1924), URL <https://link.aps.org/doi/10.1103/PhysRev.24.644>.
- [48] K. Behnia, *Fundamentals of Thermoelectricity* (Oxford University Press, 2015), ISBN 9780199697663, URL <http://www.oxfordscholarship.com/view/10.1093/acprof:oso/9780199697663.001.0001/acprof-9780199697663>.
- [49] H. B. Callen, *Phys. Rev.* **73**, 1349 (1948), URL <https://link.aps.org/doi/10.1103/PhysRev.73.1349>.
- [50] F. Rullier-Albenque, R. Tourbot, H. Alloul, P. Lejay, D. Colson, and A. Forget, *Phys. Rev. Lett.* **96**, 067002 (2006), URL <https://link.aps.org/doi/10.1103/PhysRevLett.96.067002>.
- [51] J. Chang, R. Daou, C. Proust, D. LeBoeuf, N. Doiron-Leyraud, F. Laliberté, B. Pingault, B. J. Ramshaw, R. Liang, D. A. Bonn, et al., *Phys. Rev. Lett.* **104**, 057005 (2010), URL <https://link.aps.org/doi/10.1103/PhysRevLett.104.057005>.
- [52] National Institute of Standards and Technology database, see <https://webbook.nist.gov/chemistry/fluid> (????).

A. Experimental technique

The two-thermometers-one-heater setup shown in Fig. 1b of the main text permits the measurement of all transverse and longitudinal electric and thermoelectric transport coefficients in the same conditions. A longitudinal thermal gradient $\nabla_x T$ is generated by gluing one end of the sample with silver paste to a cold finger and connecting the other end to a heater. The thermal gradient $\nabla_x T = (T_{\text{hot}} - T_{\text{cold}})/s$ was measured by two RuO₂ thermometers T_{hot} and T_{cold} attached to the sample with electric leads, separated by a distance s , that allowed as well to measure the longitudinal and transverse voltage drops, V_x and V_y , respectively. The Nernst coefficient is obtained using $N = E_y/\nabla_x T$ with $E_y = V_y/w$ and the sample width w . By applying an electric current instead of a heat current, the same experimental setup also allows to measure the longitudinal resistance and the Hall effect. The magnetic field was applied perpendicular to the orientation of both the applied heat current and the measured voltage drops. The setup was mounted on a ³He-dilution probe as well as on a home-built measurement stick for a Physical Property Measurement System (PPMS) that allowed to access temperatures down to 1.7 K.

Prior to the Nernst measurements, we determined the thermal conductivity κ of the insulating substrate by measuring the temperature gradient introduced by a measured heat current. Fig. S 5 compares the measured κ of the substrate (i.e., an insulating SrTiO₃ crystal) with previous measurements of bulk SrTiO₃ above 1.8 K [39]. The two data sets appear to join each other smoothly. This agreement confirms the accuracy of our quantification of the thermal gradient.

The presence of a sub-micronic thick δ -doped SrTi_{0.99}Nb_{0.01}O₃ sample on the substrate does not alter heat transport in any detectable way. Knowing the thermal conductivity, which remains unchanged by the application of magnetic fields smaller than 0.1 T, allowed us to quantify the Nernst signal by measuring the transverse electric field E_y produced by a specific longitudinal thermal current at a specific temperature.

B. The Nernst signal generated by short-lived Cooper pairs

Fluctuations of the superconducting order parameter above the critical temperature generate a Nernst signal. This was first theoretically described by Ussishkin, Sondhi and Huse (USH) [24] and was then elaborated in more detail and extended to finite magnetic fields by Serbyn and co-workers [25] and by Michaeli and Finkel'stein [26]. Its experimental relevance was tested in both amorphous superconductors [3, 19, 27, 40] and in high- T_c cuprates [9, 20, 21]. In this section, we compare the magnitude of the Nernst signal above T_c in the Nb-doped STO film of the present study with previous

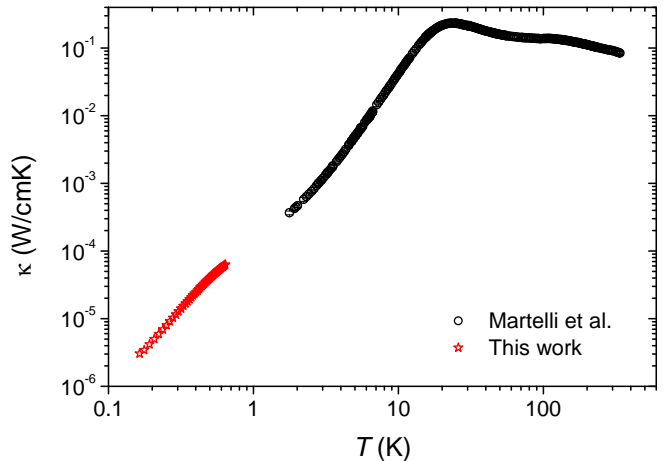


FIG. 5: **Thermal conductivity** Thermal conductivity κ as a function of temperature T in comparison to previous data on SrTiO₃ by Martelli et al. [39].

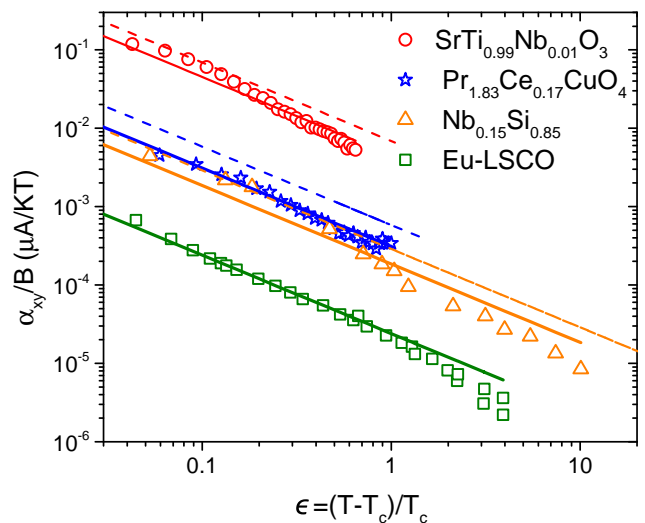


FIG. 6: **Fluctuating Nernst signal in different superconductors:** The transverse thermoelectric conductivity divided by magnetic field (α_{xy}/B) for the Nb-doped STO hetero-structure, Nb_{0.15}Si_{0.85} [19], Pr_{1.83}Ce_{0.17}CuO₄ (PCCO) [21] and La_{1.69}Eu_{0.2}Sr_{0.11}CuO₄ (Eu-LSCO) [20]. Solid lines show linear fits to the data as expected by Eqs. B1 and B2.

reports.

The USH expression for superconducting fluctuations for a 2D superconductor is remarkably simple. The off-diagonal component of the thermoelectric tensor is expected to have an additional contribution which scales with the superconducting coherence length ξ . Provided that the magnetic field is small enough (i.e., $B \ll \phi_0/2\pi\xi^2$), one expects:

$$\frac{\alpha_{xy}^{Fl}}{B} = \frac{k_B e^2}{6\pi\hbar^2} \xi^2 \quad (\text{B1})$$

The Ginzburg-Landau superconducting correlation length in the normal state [41] is:

$$\xi = \frac{\xi_0}{\sqrt{\epsilon}} \quad (\text{B2})$$

Here, ξ_0 is the temperature-independent superconducting coherence length and $\epsilon = (T - T_c)/T_c$ is the reduced temperature. Thus, the USH expression expects a fluctuating signal proportional to $1/\epsilon$.

Fig. S 6 compares the experimental $\alpha_{xy}/B(\epsilon)$ in Nb-doped STO with three other superconductors, namely $\text{Nb}_{0.15}\text{Si}_{0.85}$ [19], $\text{Pr}_{1.83}\text{Ce}_{0.17}\text{Cu}_4\text{O}$ (PCCO) [21] and $\text{La}_{1.69}\text{Eu}_{0.2}\text{Sr}_{0.11}\text{CuO}_4$ (Eu-LSCO) [20]. In all superconductors, the data roughly follows a $1/\epsilon$ -dependence confirming USH theory.

The deviation from this behavior at low ϵ may result from short wavelength effects around $\epsilon = 0.25$ [42].

According to Eq. B2, $\alpha_{xy}^{Fl}(\epsilon = 1)$ should be larger in a superconductor with longer ξ_0 . As seen in Fig. S6, this is indeed the case. The signal in Nb-doped STO is two orders of magnitude larger than in Eu-LSCO. The latter has an upper critical field which is almost two orders of magnitude larger.

It is instructive to compare the superconducting coherence lengths extracted from three distinct experimental sources:

i) The expression for the coherence length in a dirty superconductor, ξ_{0d} , extracted from Fermi velocity v_F and mean-free path ℓ , [41]:

$$\xi_{0d} = 0.36 \sqrt{\frac{3\hbar v_F \ell}{2k_B T_c}} \quad (\text{B3})$$

ii) The zero-temperature upper critical field:

$$\xi_0 = \sqrt{\frac{\phi_0}{2\pi H_{c2}(0)}} \quad (\text{B4})$$

iii) The Nernst data using equations B1 and B2:

$$\xi_N = \sqrt{\frac{6\pi\hbar^2 \alpha_{xy}^{Fl}(\epsilon = 1)}{k_B e^2 B}} \quad (\text{B5})$$

Table I presents such a comparison. As seen in the table, the three numbers are close but not identical. For Nb-doped STO, v_{Fl} was estimated via $v_{Fl} = 3\kappa/\gamma_e T = (\pi k_B/e)^2 \sigma/\gamma_e$ with the measured conductivity $\sigma = 1/\rho_{xx}$ and the electronic specific heat taken from ref. [43].

C. Entropy per vortex in doped strontium titanate

Sergeev and co-workers [12], revisiting earlier theories [10, 11], contested the validity of the following expression for the vortex transport entropy derived by Stephen [10]:

$$S_d^{EM} = -\frac{\phi_0}{4\pi} \frac{\partial H_{c1}}{\partial T} \quad (\text{C1})$$

Such an expression is derived by assuming that the entropy of the vortex is set by the temperature derivative of the energy cost to introduce a vortex at the lower critical field, H_{c1} . According to ref. [12], this energy cost includes supercurrents, which do not transport entropy. Therefore, the correct expression for entropy is:

$$S_d^{core} \simeq -\pi\xi^2 \left(\frac{\partial H_c}{\partial T}\right)^2 \quad (\text{C2})$$

Here, H_c is the thermodynamic critical field and ξ is the coherence length. S_d^{core} excludes the supercurrent contribution and is therefore smaller than S_d^{EM} by a factor of $2\ln(\frac{\lambda}{\xi})$ (λ is the penetration depth).

The lower critical field of bulk superconducting STO has been the subject of a detailed study [44]. For a sample doped with 1% of Nb ($n_{3D} = 1.9 \times 10^{20} \text{ cm}^{-3}$), it was found to be $H_{c1}(0) = 4.8 \text{ Oe}$. The $H_{c1}(T)$ curve allows to extract the slope $(\frac{\partial H_{c1}}{\partial T}(T = 0.2k) = -25 \text{ Oe/K})$. Inserting this in Eq. C1, one finds :

$$S_d^{EM} = 5.2 \times 10^{-12} \text{ J/K. m} \quad (\text{C3})$$

The Ginzburg-Landau parameter of STO at this carrier concentration was estimated to be $\frac{\lambda}{\xi} \simeq 8.5$ [44]. Thus, the core entropy S_d^{core} would be $2\ln \kappa \simeq 4.3$ times smaller :

$$S_d^{core} \approx 1.2 \times 10^{-12} \text{ J/K. m} \quad (\text{C4})$$

This is close to a generic estimation by Sergeev *et al.* [12] ($S_d^{EM} = 1.6 \times 10^{-7} \text{ erg/K. cm}$). It is also forty times larger than what the experiment would imply if one combines the measured amplitudes of the Nernst signal and resistivity ($S_d(exp.) \approx 3 \times 10^{-14} \text{ J/K. m}$), which was discussed in the main text. This discrepancy calls for a re-examination of the standard picture.

D. The Ettingshausen effect and its non-universal amplitude

The Ettingshausen coefficient is the transverse thermal gradient caused by the application of a longitudinal charge flow: $E_{tt} = \frac{\nabla_y T}{J_x}$. In a pioneering study of thermomagnetic effects in cuprates, Palstra and co-workers directly measured the Ettingshausen coefficient of optimally-doped YBCO up to $B=12 \text{ T}$ [5]. Their data is shown in Fig. S 7.

The Bridgman relation [47, 48] is the off-diagonal counterpart of the Kelvin relation and is derived from the Onsager reciprocity [49]. It links the Ettingshausen coefficient, the Nernst coefficient and the thermal conductivity, κ :

TABLE I: **A comparison of four superconductors:** Physical properties of superconductors in which a fluctuating Nernst signal above T_c has been detected. The superconducting coherence length has been extracted using three distinct equations Eq. B3, Eq. B4 and Eq. B5.

Compound	T_c [K]	H_{c2} [T]	$v_F l$ [m ² /s]	ξ_0 [nm]	ξ_{0d} [nm]	ξ_N [nm]
SrTi _{0.99} Nb _{0.01} O ₃ (present study)	0.32	0.085	9.3×10^{-4}	62	64	52
Nb _{0.15} Si _{0.85} [27]	0.38	1.1	4.35×10^{-5}	17	13	10
Pr _{1.83} Ce _{0.17} Cu ₄ O (PCCO) [21]	19.5	3	4.5×10^{-3}	10	18	14
La _{1.69} Eu _{0.2} Sr _{0.11} CuO ₄ (Eu-LSCO) [20]	3.86	6	-	7	-	3.8

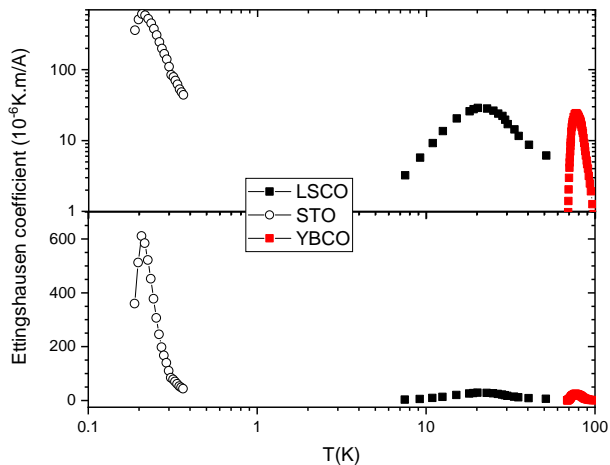


FIG. 7: **The Ettingshausen coefficient in three different superconductors:** The temperature dependence of the Ettingshausen coefficient in STO and LSCO, using the Nernst data shown in Fig. 1 of the main text, the published thermal conductivity data [45, 46] and the Bridgman relation. Also shown is the directly measured Ettingshausen coefficient in optimally doped YBa₂Cu₃O₇ [5]. Upper and lower plots show the same data in logarithmic and linear scales.

$$E_{tt} = \frac{NT}{\kappa} \quad (D1)$$

In the case of YBCO, the combination of the Ettingshausen and the Nernst data reported in ref. [5], points to a Nernst peak of $4 \mu\text{V}/\text{K}$ comparable with what has been directly measured [6, 50, 51].

Inversely, one can use the Bridgman relation to extract the Ettingshausen coefficient from the Nernst data. In La_{1-x}Sr_xCuO₂, the Nernst data ($x = 0.08$) [31] combined with the thermal conductivity data at slightly lower doping ($x = 0.04$) [45] allows one to quantify the Ettingshausen coefficient. Using the thermal conductivity of optimally-doped STO [46] and our present Nernst data, we can also quantify the Ettingshausen coefficient and its

peak value in STO. As seen in Fig. S 7, the latter peak is twenty times larger than what is seen in cuprates. This is

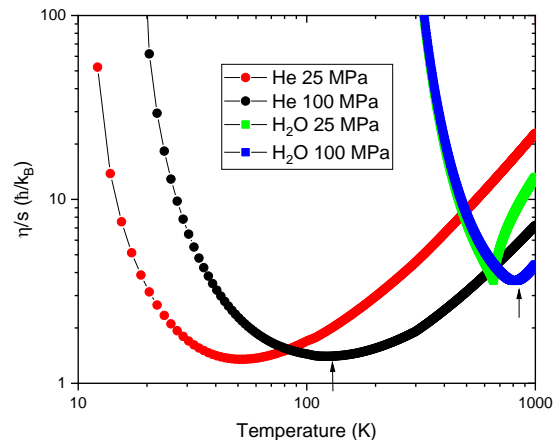


FIG. 8: **η/s ratio in supercritical liquids:** The temperature dependence of the ratio of dynamic viscosity to entropy density in H₂O and ⁴He and H₂O at two different pressures [52]. In both cases there is a minimum in η/s larger than \hbar/k_B which remains roughly the same at both pressures.

in sharp contrast with the Nernst peak which has a comparable magnitude in the two family of superconductors.

E. Bound to the viscosity-entropy ratio in common liquids

The existence of a minimum in the ratio of viscosity to entropy density of common liquids is visible in the available data [52] shown in Fig. S 8 for two supercritical liquids, namely ⁴He and H₂O. In both, $\eta/s(T)$ has a minimum which is 1.3 (3.3) \hbar/k_B in He (H₂O). A recent theoretical work [14] has argued that this minimum arises because of a universal bound to the kinematic viscosity of liquids.